Turk J Elec Engin, VOL.10, NO.2 2002, © TÜBİTAK

Development of a Cylindrical Waveguide Antenna Array with a High Isolation Between Receive - Transmit Sub arrays: Theory and Experiment

Vladimir I. OKHMATOVSKY
Department of Antennas and Radio Waves Propagation,
Moscow Power Engineering Institute, Moscow-RUSSIA
Konstantina S. NIKITA, Stavros KOULOURIDIS and Nikolaos K. UZUNOĞLU
Department of Electrical and Computer Engineering, National
Technical University of Athens-GREECE

Abstract

The possibility of developing an antenna system consisting of transmit and receive arrays and being able to work simultaneously in full duplex mode at the same frequency is a very attractive task. This could only be achieved if the isolation between the transmit and receive arrays is sufficiently high not to cause a parasitic oscillation which will ruin the proper operation of a transponder system to which the arrays will be connected.

Specifically, in this paper the operation of two peripheral open waveguide arrays placed on a cylindrical surface and being isolated with a radial line operating as a space filter, is studied. In analyzing the radiation properties of this rather complicated array antenna which has a conformal structure, an integral equation technique is used, while the solution of the derived set of equations is obtained by using a Galerkin approach. The accuracy of the developed solution is verified by several tests such as energy conservation theorem, convergence patterns and comparison with results obtained by applying the physical theory of diffraction technique. In addition to the theoretical analysis, an experimental antenna system has been developed and measured. Comparison of theoretical and experimental results is carried out and the validity of the solution is verified.

Key Words: *cylindrical waveguide, aperture antenna, Galerkin method, antenna array, transmit and receive sub-arrays, space filters, loaded radial line, boundary value problem, Dyadic Green's function*

1. Introduction

In many telecommunication, radar and transponder systems, it is highly desirable to achieve simultaneous reception and transmission at the very same frequency. In practice, this is a highly difficult task and traditionally frequency multiplexing or time division multiplexing techniques are employed. This fundamental requirement is shown in Figure 1, where the basic associated phenomena are indicated. Indeed, if no care is taken, the whole system enters into a self oscillation mode at the most preferred frequency, depending on the transfer function characteristics of the chain consisting of the reception antenna, the active element (amplifier) transmit antenna and the air medium between the two antennas. It is evident that if the active element amplifier has a gain of G (dB), then the isolation (or attenuation) between the input and the output

of the two antennas must be $I \leq -G(dB) - L_e$, where L_e is a safety margin to avoid parasitic oscillations. Assuming a reception signal level of -50 dBm and a transmit power of 40 dBm, then taking the reasonable value of $L_e = 6\,dB$, it is necessary to have $I \leq -96\,dB$. Therefore, a relatively high decoupling between the two antenna elements is needed. In investigating further this issue, one can easily state the two fundamental mechanisms determining the coupling or equivalently the isolation between the two coupled antenna units:

a) Direct coupling between the receive/transmit antennas

b) Increase of the coupling due to reflections from neighboring objects.

In the effort to reduce the overall isolation, one has to cope with the reflection from neighboring scatterers (coupling mechanism (b)) by covering the scatterers using absorbing materials and/or by suppressing the side lobes of the antenna itself. In treating the mechanism (a), the direct coupling between receive/transmit antennas, the use of space filters has been proposed in the past. In this paper, a loaded radial line is proposed to decrease the direct coupling between receive/transmit subarrays as shown in Figure 2, where peripheral subarrays consisting of open waveguide aperture elements are arranged in two rows on a cylindrical conductor. A radial line is placed between the two rows of subarrays and the radial line is terminated with an absorbing material described with a surface impedance boundary condition which is specified in the next section. The waveguide array elements are of orthogonal type and each subarray consists of an arbitrary number of L elements. In Figure 2, the symbols used to define the structure are defined.

In the following, an $\exp(+j\omega t)$ time dependence is assumed and is suppressed throughout the analysis.

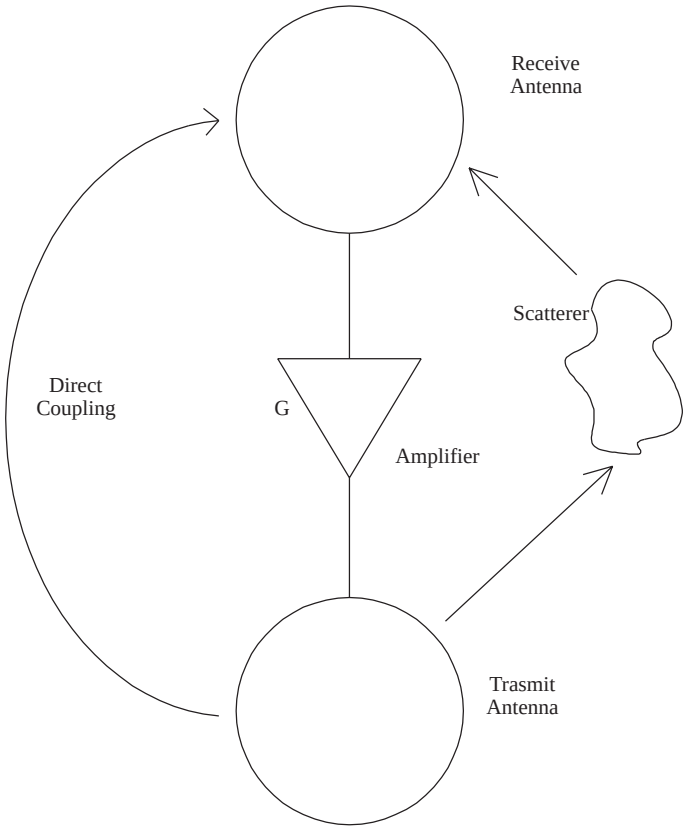

Figure 1. Transporter operation principle

2. Formulation of the Boundary Value Problem

In order to proceed to the formulation of the radiation structure defined in Figure 2, an integral equation approach will be pursued. It is assumed that each waveguide is excited with an incident wave of known amplitude and phase. In the first place, the exterior space of the cylindrical antenna is considered. In Figure 3, the cross section of the outer space region is shown, to make easier the presentation of the proposed formulation. According to the equivalence principle, at an arbitrary point $\underline{p}$ inside the volume V_{ext} (see Figure 3), the electric and magnetic fields can be expressed in terms of the equivalent electric and magnetic currents on the surface S, shown also in Figure 3. According to this,

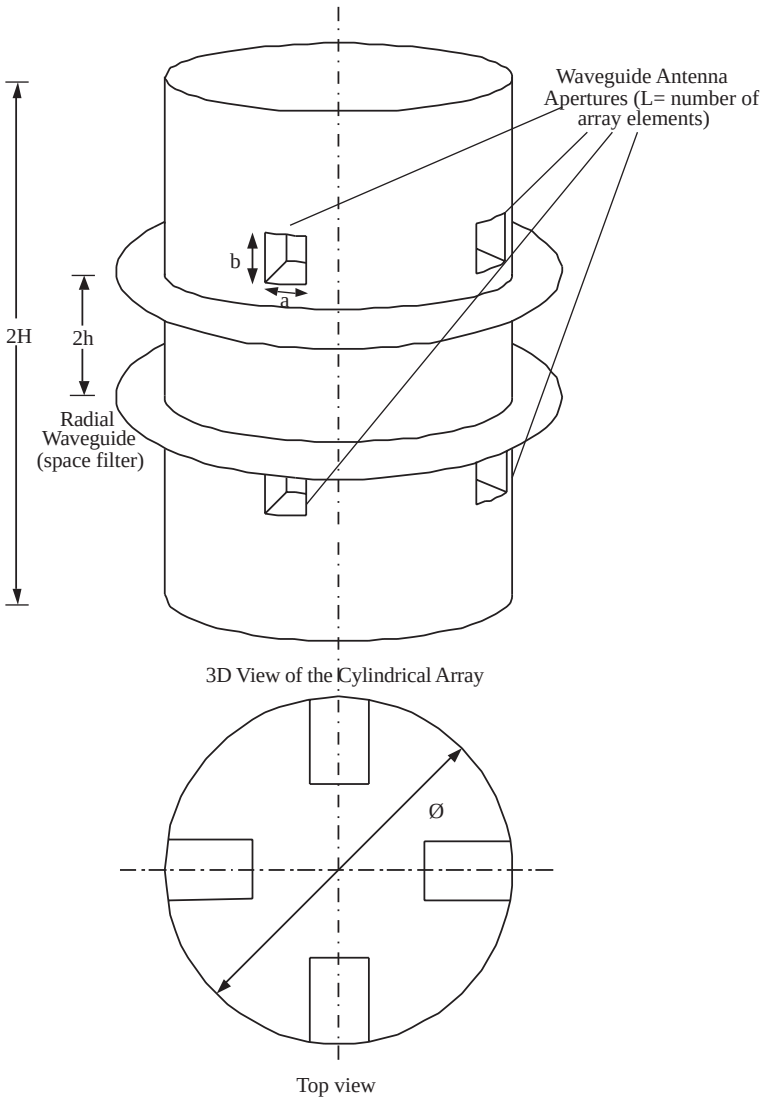

Figure 2. Cylindrical waveguide antenna array structure

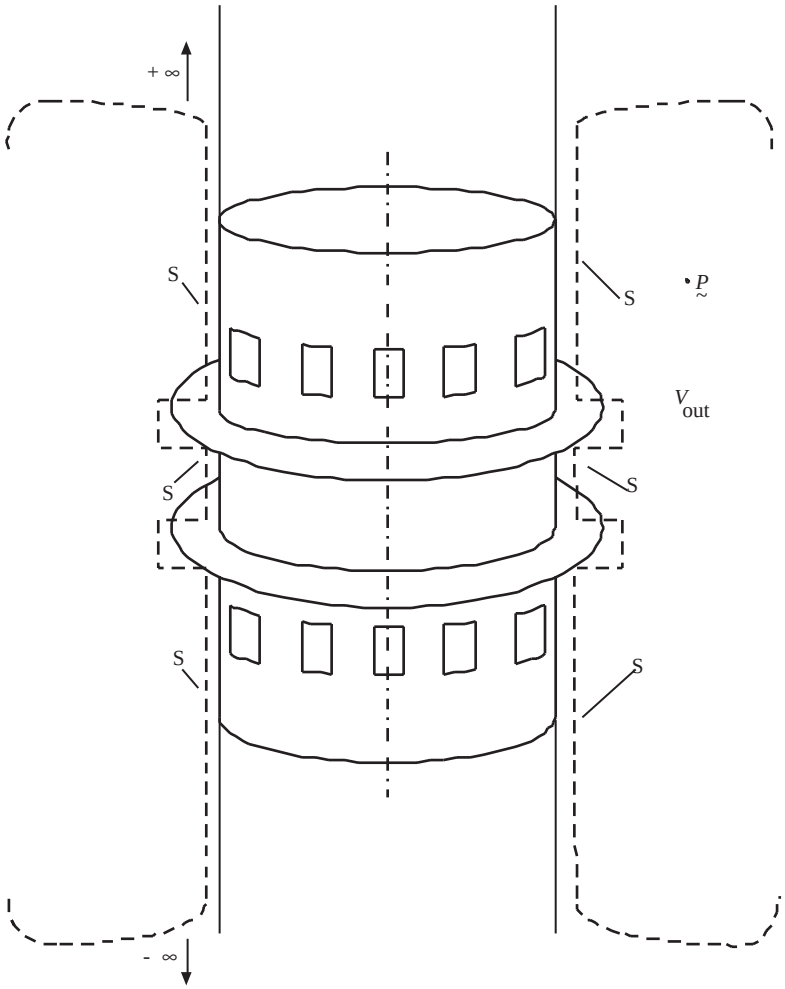

Figure 3. Implementation of Green's Theorem to obtain integral equations.

$$\begin{aligned}\underline{E}_e(\underline{p}) = \; & -\sum_{\ell=1}^{2L} \iint_{S_\ell} \underline{J}^m(\underline{q}) \cdot \bar{\underline{G}}^{me}(\underline{q},\underline{p}) ds_q + \int\int_{S_{ann+}} \underline{J}^e(\bar{q}) \cdot \bar{\underline{G}}^{ee}(\underline{q},\underline{p}) ds_q \\ & + \int\int_{S_{ann-}} \underline{J}^e(\underline{q}) \cdot \bar{\underline{G}}^{ee}(\underline{q},\underline{p}) ds_q - \iint_{S_{imp}} \underline{J}^e(\underline{q}) \cdot \bar{\underline{G}}^{ee}(\underline{q},\underline{p}) ds_q \end{aligned} \tag{1}$$

$$\begin{aligned}\underline{H}_e(\underline{p}) = \; & \sum_{\ell=1}^{L} \iint_{S_\ell} \underline{J}^m(\bar{q}) \cdot \bar{\underline{G}}^{mm}(\underline{q},\underline{p}) ds_q - \int\int_{S_{ann+}} \underline{J}^e(\underline{q}) \cdot \bar{\underline{G}}^{em}(\underline{q},\underline{p}) ds_q \\ & - \int\int_{S_{ann-}} \underline{J}^e(\underline{q}) \cdot \bar{\underline{G}}^{em}(\underline{q},\underline{p}) ds_q + \iint_{S_{imp}} \underline{J}^m(\underline{q}) \cdot \bar{\underline{G}}^{em}(\underline{q},\underline{p}) ds_q \end{aligned} \tag{2}$$

where

$\bar{\underline{G}}^{ee}(\underline{q},\underline{p})$ is the dyadic infinite cylinder electric field / electric source Green's function

$\bar{\underline{G}}^{em}(\underline{q},\underline{p})$ is the dyadic infinite cylinder electric field / magnetic source Green's function

$\bar{\underline{G}}^{me}(\underline{q},\underline{p})$ is the dyadic infinite cylinder magnetic field / electric source Green's function

$\bar{\underline{G}}^{mm}(\underline{q},\underline{p})$ is the dyadic infinite cylinder magnetic field / magnetic source Green's function

The current sources $\underline{J}^e(\underline{q}_s) = \hat{n} \times \underline{H}(\underline{q}_s)$ and $\underline{J}^m(\underline{q}_s) = -\hat{n} \times \underline{E}(\underline{q}_s)$ are referred to:

S_ℓ $(\ell = 1, 2, ..., L, ..., 2L)$ - the waveguide aperture surfaces

S_{ann+}, S_{ann-} – the surfaces of the radial waveguide up and down perfect conductors (see Figure 3)

S_{imp} – the cylindrical surface terminating the radial line (see Figure 3).

The expressions for the Green's dyadics $\bar{\underline{G}}^{ee}(\underline{q}, \underline{p})$, $\bar{\underline{G}}^{em}(\underline{q}, \underline{p})$, $\bar{\underline{G}}^{me}(\underline{q}, \underline{p})$ and $\bar{\underline{G}}^{mm}(\underline{q}, \underline{p})$ are obtained using the method of separation of variables based on techniques presented in [1].

As a second step, the regions inside the waveguides are considered. Applying the same principles as in Eqs. (1) and (2) for the region inside the waveguides and incorporating the corresponding dyadic Green's functions for the rectangular cross section waveguide, the following equations are set:

$$\underline{E}_i^\ell(\underline{p}) = \underline{E}_{inc}^\ell(\underline{p}) + \iint_{S_\ell} \underline{J}^e(\underline{q}) \cdot \bar{\underline{g}}^{ee}(\underline{q}, \underline{p}) ds_q - \iint_{S_\ell} \underline{J}^m(\underline{q}) \cdot \bar{g}^{me}(\underline{q}, \underline{p}) ds_q \tag{3}$$

$$\underline{H}_i^\ell(\underline{p}) = \underline{H}_{inc}^\ell(\underline{p}) - \iint_{S_\ell} \underline{J}^e(\underline{q}) \cdot \bar{\underline{g}}^{em}(\underline{q}, \underline{p}) ds_q + \iint_{S_\ell} \underline{J}^m(\underline{q}) \cdot \bar{g}^{mm}(\underline{q}, \underline{p}) ds_q \tag{4}$$

where $\ell = 1, 2, ..., L, ..., 2L$, and the equivalent magnetic $(-\underline{J}^m(\underline{q}))$ and electric $(-\underline{J}^e(\underline{q}))$ currents are identical with those in Eqs. (1)-(2), while $\underline{E}_{inc}^\ell(\underline{p})$ and $\underline{H}_{inc}^\ell(\underline{p})$ are the incident wave electric and magnetic fields, respectively. Usually the incident wave fields correspond to the dominant mode TE_{10} mode, since the rectangular waveguides dimensions are selected to propagate a single mode. Note that the dyadic Green's functions $\underline{\overline{g}}^{ee}$, $\underline{\overline{g}}^{em}$, $\underline{\overline{g}}^{me}$, $\underline{\overline{g}}^{mm}$, satisfying the boundary conditions on the inner surface of waveguides, do not contribute to the right hand side of Eqs. (3) and (4) and only the open ended aperture surfaces of the waveguides appear in these equations.

In order to obtain the integral equations, the following boundary conditions should be imposed:

(a) Continuity of the tangential electric and magnetic field components on the waveguide apertures S_ℓ $(\ell = 1, 2, ..., 2L)$.

(b) Vanishing of the tangential electric field components (E_ρ and E_φ – see Figure 2) on the radial line upper and lower surfaces.

(c) Satisfaction of Leontovich boundary conditions [3] the termination of the cylindrical radial waveguide on the $\rho = a$ cylinder surface (see Figure 2). The exact boundary conditions are expressed as follows:

$$\underline{E}_e \cdot \hat{z} = \dot{Z} \underline{H}_e \cdot \hat{\varphi} \tag{5}$$

$$\underline{E}_e \cdot \hat{\varphi} = -\dot{Z} \underline{H}_e \cdot \hat{z} \tag{6}$$

where $\hat{z}$ and $\hat{\varphi}$ are the unit vectors along the polar coordinates z and φ, while $\dot{Z}$ is the complex surface impedance.

It should be emphasized that the use of the proper Green's dyadic restrict the integral equations to the above mentioned surfaces in satisfying the conditions (a), (b), and (c). The unknown functions appearing in the integral equations are:

- Tangential electric fields on the open waveguide apertures. Note that once the electric field is known, then the magnetic field is also known.

- Electric currents on the radial waveguide upper and lower annular shape conducting walls (taken with zero thickness)

- Tangential electric field components ($E_{ez} = \underline{E}_e \cdot \hat{z}$ and $E_{e\varphi} = \underline{E}_e \cdot \hat{\varphi}$) on the absorbing material, placed as a termination of the radial line.

In the following section, solution of the obtained system of integral equations, based on the Galerkin technique, is proposed and delineated.

3. Solution of the Integral Equations: Galerkin Method

In order to solve the system of integral equations set up in the previous section and compute the radiation properties of the structure under investigation, the Galerkin technique has been pursued. Along this direction, the unknown field quantities appearing in the integral equations should be described in terms of proper 'describing' functions. Then, the set of integral equations are converted to a linear system of equations by taking the inner product of the equations with testing functions being identical with the 'describing' functions. It is known that this procedure, being a subclass of Method of Moments techniques, provides an excellent numerical stability. Therefore, the key issues to be addressed are:

a) Best selection of 'describing' functions satisfying physical conditions corresponding to specific electric and magnetic currents.

a) Efficient calculation of the matrix elements arising in applying Galerkin technique.

After a review of the physical conditions, the following 'describing' functions were selected.

A. Electric and magnetic currents on the waveguide apertures

The complete set of Transverse Electric (TE) and transverse Magnetic (TM)) modes has been used to expand the electric and magnetic currents on the waveguide apertures. The effectiveness of using these describing functions to express the open waveguide aperture fields has already been proved [4] and is evident. Note that by expressing the dyadic Green's functions of the waveguides in terms of the same modes and making use of the orthogonality relations [4], the diagonal terms – being also dominant terms – are easily computed. The coupling matrix elements between the waveguide apertures are computed also analytically, since products of trigonometric functions are encountered. In this context, a geometrical approximation of the circular waveguide apertures to orthogonal shape is implemented to facilitate the computation of the associated integrals, that is the arc length of the circular horizontal dimension of the waveguide is assumed to be a linear segment [5].

B. Electric current description on annular radial line conductors

In selecting the proper describing functions for the current distribution on the two radial waveguides annular upper and lower surfaces, the edge conditions on the $\rho = R_1$, $z = \pm h_r$ are taken into account to accelerate

the convergence of the obtained solution. Taking into account the requirement of easy computation of the corresponding matrix elements, a polynomial type expansion is selected as follows:

$$J_{\rho}^{e\pm}(\rho,\varphi)=\sqrt{1-(\frac{\rho}{R_1})^2}\sum_{p=-\underline{P}}^{\underline{P}}\sum_{q=0}^{Q}C_{pq}^{\rho\pm}e^{jp\varphi}\rho^q \tag{6}$$

$$J_{\varphi}^{e\pm}(\rho,\varphi)=\frac{1}{\sqrt{1-(\frac{\rho}{R_1})^2}}\sum_{p=-\underline{P}}^{\underline{P}}\sum_{q=0}^{Q}C_{pq}^{\varphi\pm}e^{jp\varphi}\rho^q \tag{7}$$

where $C_{pq}^{\rho\pm}$,$C_{pq}^{\varphi\pm}$ are unknown coefficients to be determined and the $\pm$ superscripts are used to denote the current on the upper (S_{ann+}) and lower (S_{ann-}) radial waveguide conducting surfaces (see Figure 2). Note that the infinite conducting cylinder dyadic Green's function being expressed in terms of cylindrical wave functions with radial dependence given by Bessel functions, the involved integrals in the process of inner products are computed by using power series and relevant asymptotic expansions of Bessel functions.

C. Magnetic current distribution on the radial waveguide termination

In order to describe the magnetic current (or electric field) distribution on the cylindrical surface of the radial waveguide, the boundary conditions on the upper and lower annular walls are taken into account. That is,

$$E_{\rho}(a,\varphi,z)|_{z=\pm h}=0 \text{ or } \frac{\partial E_z(a,\varphi,z)}{\partial z}|_{z=\pm h}=0 \tag{8}$$

and

$$E_{\varphi}(a,\varphi,z)|_{z=\pm h}=0. \tag{9}$$

Then, the following expansions are adopted:

$$J_{\varphi}^{m}(\varphi,z)=\sum_{n=-N}^{N}\sum_{m=0}^{M}U_{nm}e^{jn\varphi}\cos(\frac{m\pi(z+h)}{2h}) \tag{10}$$

$$J_{\rho}^{m}(\varphi,z)=\sum_{n=-N}^{N}\sum_{m=1}^{M}V_{nm}e^{jn\varphi}\sin(\frac{m\pi(z+h)}{2h}). \tag{11}$$

Again the selection of the above sinusoidal describing functions with respect to the z- axis facilitates the computation of the generalized admittance matrix elements, since the dyadic Green's functions has an $\exp(jk(z-z'))$ dependence, with k being the spectral variable and $(z-z')$ the distance between the observation (z) and the source (z') points along the z – axis.

Note that for both annular conductors (S_{ann+} and S_{ann-}) and impendance boundary surface (S_{imp}), the use of trigonometric expansions $e^{jm\varphi}$ to azimuthal angle is taken.

4. Computation of the Generalized Admittance Matrix Elements

Because of the very complex geometry of the antenna array under study, the corresponding system matrix is extremely complex and is not given here explicitly. In computing the involved matrix elements, all the integrals associated with the spatial coordinates (φ and z on the waveguide apertures and impedance surface, r and φ on the annular radial waveguide walls) are computed analytically.

Then, the computation of the resulting matrix elements involves infinite summations related to rectangular waveguide Green's dyadics, an infinite spectral integral $\int_{-\infty}^{+\infty} dk$ (along the z axis of the phase space) and an infinite summation over the azimuthal ($\exp(\mathrm{jm}\varphi)$) integer variable.

In computing the infinite summations, convergence tests were carried out to achieve desired accuracy, while for the case of the infinite integral $\int_{-\infty}^{+\infty} dk$ computation, truncation of upper and lower bounds was implemented after a careful investigation of integrand functions, which is also used to define a sufficient number of sampling points in the course of numerical integration. In all cases, strict convergence tests were carried out to guarantee the accurate computation of the matrix elements. Furthermore in computing the $\int_{-\infty}^{+\infty} dk$ integrals and in order to improve convergence of the integrals asymptotic parts of the ratios of Bessel functions their derivatives were introduced and then a technique similar to the Kummer's transformation is applied to compute the involved series. Also the singularities associated with the branch points and Bessel functions in the vicinity of k=0 were taken into account analyticaly.

After computing the matrix elements, the resulting linear system of equations is solved using LU decomposition technique.

5. Numerical Computations

A software program has been developed, based on the theory presented briefly in the previous sections. In order to check and verify the accuracy of the code, independent checks were carried out such as:

(a) Validity of the energy conservation principle. The radiated power by the whole system is compared to the net power entering the waveguides.

(b) Comparison of the computed current distribution on the radial waveguide annular upper and lower walls with the results obtained by applying the physical theory of diffraction.

Both checks provided satisfactory results.

6. Experimental System

An experimental antenna system has been designed and constructed. A photography of the system is presented in Figure 4. The number of array elements was 2L=8 and the operating frequency was f=10.0 GHz. The waveguides were excited with a standard coaxial to waveguide transition. The cylindrical surface within the radial line of 2h in height was covered with a commercially absorbing material (ECCOSORB®SFU by Emerson & Cuming). The experimental antenna dimensions are Φ=160 mm, 2H=280 mm, 2h=30 mm, a=23 mm, b=23 mm.

Figure 4. Photography of experimental Antenna.

Measurements of S parameters of the antenna were carried out while matching all the antenna feeds by Z_O=50 Ohm loads. In Figures 5, 6 experimental results of measured $|S|$ parameters are shown in the frequency region 9.50-10.50 GHz. In each case the input/output port are shown for the cases when absorbing material is used or not. On the same figures the theoretical computed values are shown. It is shown that the theory predicts to a sufficient degree the isolation level between the various array elements. Both theoretical and experimental results exhibit the possibility of achieving –50 dB isolation between vertically displaced array elements. The significance of using absorbing material is also demonstrated.

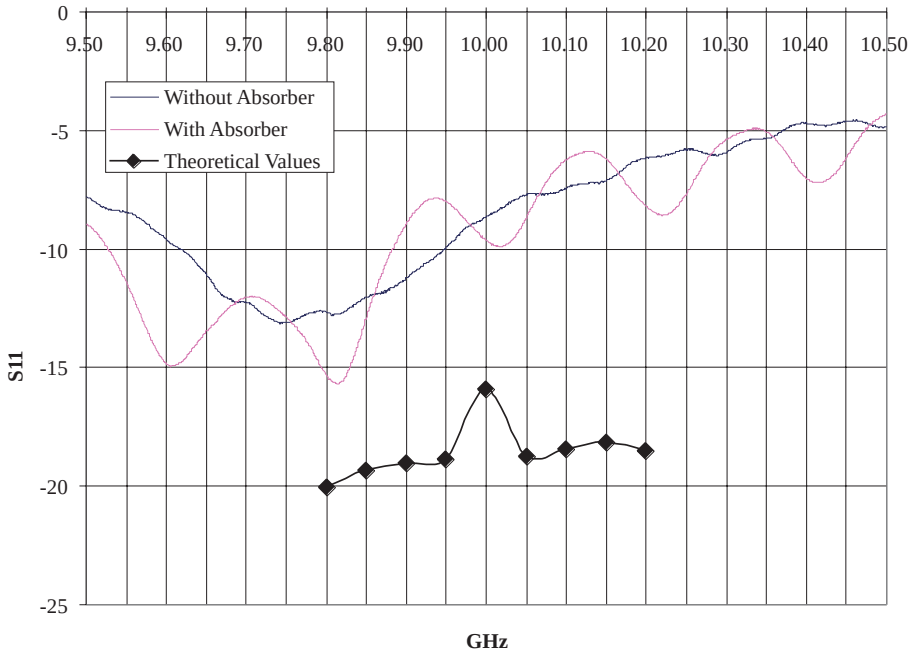

Figure 5. Experimental and theoretical values for the waveguide antenna for$|S_{11}|$ for an array element. Values are in dB.

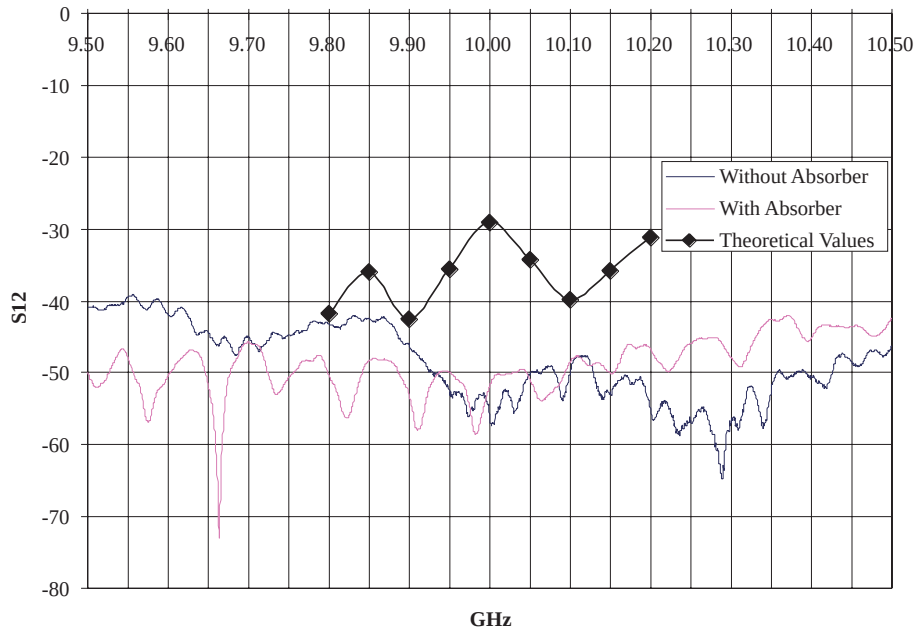

Figure 6. Experimental and theoretical values for the waveguide antenna for$|S_{21}|$ for vertically displaced array elements Values are in dB.

7. Conclusions

A circular waveguide array incorporating transmit and receive antenna elements placed above and below a space filter has been analyzed by applying a rigorous analysis based on integral equations. A careful selection of describing testing functions in the framework of a Galerkin technique is applied to obtain the solution. Extensive tests to verify the accuracy of the method are utilized. An experimental antenna of 8 elements were constructed and measured. Comparison of theoretical and experimental results shows good agreement and also shows the ability to obtain an optimized isolation between transmit and receive subarrays.

References

[1] C. T. Tai, *Dyadic Green's Functions in Electromagnetic Theory*, Scranton, PA: Intext, 1971.

[2] Carry C. Hess, "Land Mobile Radio System Engineering", *Arctech House*, Boston, 1993.

[3] D. S. Jones, "Theory of Electromagnetism", *Pergamon Press*, 1964.

[4] K. S. Nikita and N. K. Uzunoglu, "Analysis of the Power Coupling from a Waveguide Hyperthermia Applicator into a Three-layered Tissue", *IEEE Transactions on Microwave Theory and Techniques*, vol. MTT-37, pp. 1794-1801, 1989.

[5] K. S. Nikita and N. K. Uzunoglu, "Coupling Phenomena in Concentric Multi-Applicator Phased Array Hyperthermia Systems", *IEEE Transactions on Microwave Theory and Techniques*, vol. 44, pp. 65-74, 1996.